Proceedings of the ASME 2015 International Design Engineering Technical Conferences & Computers and Information in Engineering Conference
IDETC/CIE 2015
August 2-5, 2015, Boston, Massachusetts, USA

DETC2015-47677

QUANTIFICATION OF MODEL-FORM UNCERTAINTY IN DRIFT-DIFFUSION SIMULATION USING FRACTIONAL DERIVATIVES

Yan Wang
School of Mechanical Engineering
Georgia Institute of Technology
Atlanta, GA 30332

ABSTRACT

In modeling and simulation, model-form uncertainty arises from the lack of knowledge and simplification during modeling process and numerical treatment for ease of computation. Traditional uncertainty quantification approaches are based on assumptions of stochasticity in real, reciprocal, or functional spaces to make them computationally tractable. This makes the prediction of important quantities of interest such as rare events difficult. In this paper, a new approach to capture model-form uncertainty is proposed. It is based on fractional calculus, and its flexibility allows us to model a family of non-Gaussian processes, which provides a more generic description of the physical world. A generalized fractional Fokker-Planck equation (fFPE) is proposed to describe the drift-diffusion processes under long-range correlations and memory effects. A new model calibration approach based on the maximum accumulative mutual information is also proposed to reduce model-form uncertainty, where an optimization procedure is taken.

1. INTRODUCTION

Two types of uncertainty are recognized in modeling and simulation. Aleatory uncertainty is due to pure randomness of physical world, whereas epistemic uncertainty is because of the lack of complete knowledge about the world. The major component of epistemic uncertainty is model-form uncertainty, which arises from the simplification during modeling process and numerical treatment for ease of computation. During the abstraction procedure, truncation is always applied to make simulation and computation tractable. As a result, error or bias is introduced. The difference between the model prediction of a quantity of interest (QoI) and its true value in the real physical world is the accumulative effect of model-form uncertainty and other input uncertainties such as variability and bias in the parameters and variables.

Classical uncertainty quantification (UQ) methods to model output uncertainty propagated from inputs, such as generalized polynomial chaos [1], moment and characteristic function [2], have relatively restrictive assumptions of stochasticites, i.e. the types of distributions to sample and the forms of polynomials in expansion. These methods are very effective in analyzing systems with low-dimensional parameter space that follow simple physics. However, when we are interested in multi-physics systems with nonlocal long-range correlations and memory effects, or extreme events under heavy-tailed distributions, these UQ methods can lead to inaccurate conclusion because the distributions have the bias toward traditional Gaussian process. The error is largely due to the selected model form. Although methods such as Bayesian model average are available to calibrate the model, they rely on the assumptions that all possible models and the corresponding probabilities that the models are correct are readily available.

In this paper, a new UQ method is proposed to describe multi-physics systems with model-form uncertainty incorporated, where the physics does not follow traditional partial differential equation (PDEs) or ordinary differential equations (ODEs). It is based on the concept of fractional calculus. Fractional calculus [3,4] is a generalization of classical real analysis by introducing non-integer power and differentiation operators. As a result, classical differentiation equations that model system dynamics can be extended to fractional differentiation equations with fractional derivatives defined. Fractional calculus has been applied in the regimes of system dynamics and control [5], mechanics of quasi-brittle materials [6], non-local continuum and viscoelastic mechanics [7], time-space fractional diffusion equation [8,9], fractional Fokker-Planck equation [10,11], and fractional Schrödinger equation [12]. The uniqueness of fractional diffusion equation is that the solution can be deviated from the Gaussian process

as in traditional diffusion equation. Therefore, heavy tails as in Lévy α-stable white noise processes can be obtained. Similarly, fractional Fokker-Planck equation with fractional derivatives models Lévy flights. Fractional Schrödinger equation generalizes the classical description of quantum system dynamics with Lévy stochastic process.

Based on fractional calculus, a generalized fractional Fokker-Planck equation is proposed in this paper to describe the general drift-diffusion process with multi-physics complexity. This approach does not need the assumption of the possible choices of models and associated probabilities. Rather, the form of model may vary dynamically based on the control of several parameters. In other words, the model form may change parametrically during simulation.

In addition, the flexibility of the fractional Fokker-Planck equation allows us to represent the evolution of probability distributions with heavy tails, since the results of fractional calculus can be geometrically interpreted as fractals, physically as long-range interaction or long-term memory, and probabilistically as heavy-tailed stable distributions. Rare event with extreme impact has been a classical interest in statistics. Extreme value distribution functions [13,14] (e.g. Fréchet, Gumbel, and negative Weibull) are typically used in modeling long tails. Yet, they are general enough to capture the variation of the distribution form. In this paper, a new model calibration approach is proposed to reduce model-form uncertainty. It is based on the mechanism of maximizing a new criterion, accumulative mutual information, such that the accumulative difference between the target distribution and the predicted probability evolution from the fractional Fokker-Planck equation is minimized.

In the remainder of the paper, fractional calculus is introduced in Section 2. The generalized fractional Fokker-Planck equation is proposed and the analytical solution is provided in Section 3. The sensitivity analysis based on the analytical solution for drift-diffusion processes is presented in Section 4.1. The new model calibration approach is described in Section 4.2.

2. FRACTIONAL DERIVATIVES

Several forms of fractional integrals and derivatives have been developed. The definitions of left and right Riemann-Liouville fractional integrals are

$$D_{+}^{-\alpha} f(x) = \frac{1}{\Gamma(\alpha)} \int_{-\infty}^{x} (x-\xi)^{\alpha-1} f(\xi) d\xi \tag{1}$$

and

$$D_{-}^{-\alpha} f(x) = \frac{1}{\Gamma(\alpha)} \int_{x}^{+\infty} (\xi-x)^{\alpha-1} f(\xi) d\xi \tag{2}$$

respectively.

The definitions of left and right Riemann-Liouville fractional derivatives are

$$D_{+}^{\alpha} f(x) = \frac{1}{\Gamma(n-\alpha)} \frac{d^n}{dx^n} \int_{-\infty}^{x} (x-\xi)^{n-\alpha-1} f(\xi) d\xi \tag{3}$$

and

$$D_{-}^{\alpha} f(x) = \frac{(-1)^n}{\Gamma(n-\alpha)} \frac{d^n}{dx^n} \int_{x}^{+\infty} (\xi-x)^{n-\alpha-1} f(\xi) d\xi \tag{4}$$

where integer $n = \lfloor \alpha \rfloor$ or $n \le \alpha < n+1$.

The Riesz fractional integral is defined as

$$D^{-\alpha} f(x) = \frac{1}{2\cos(\alpha\pi/2)} [D_{+}^{-\alpha} f(x) + D_{-}^{-\alpha} f(x)] \tag{5}$$

and the Riesz fractional derivative is defined as .

$$D^{\alpha} f(x) = -\frac{1}{2\cos(\alpha\pi/2)} [D_{+}^{\alpha} f(x) + D_{-}^{\alpha} f(x)] \tag{6}$$

The Fourier transform of Riemann-Liouville and Riesz fractional derivatives are

$$\mathcal{F}\{D_{\pm}^{\alpha} f(x); k\} = (\mp ik)^{\alpha} \mathcal{F}\{f(x); k\} \tag{7}$$

and

$$\mathcal{F}\{D^{\alpha} f(x); k\} = -|k|^{\alpha} \mathcal{F}\{f(x); k\} \tag{8}$$

respectively with $\alpha > 0$ and $i^2 = -1$, where

$$\mathcal{F}\{f(x); k\} = \hat{f}(k) = \int_{-\infty}^{+\infty} e^{ikx} f(x) dx \quad (k \in \mathbb{R}) \tag{9}$$

and

$$\mathcal{F}^{-1}\{\hat{f}(k); x\} = f(x) = \frac{1}{2\pi} \int_{-\infty}^{+\infty} e^{-ikx} \hat{f}(k) dk \quad (x \in \mathbb{R}) \tag{10}$$

Notice that

$$(\mp ik)^{\alpha} = |k|^{\alpha} e^{\mp i \,\mathrm{sgn}(k)\alpha\pi/2} \tag{11}$$

and $\mathrm{sgn}(x) = 1$ if $x > 0$, $\mathrm{sgn}(x) = 0$ if $x = 0$, and $\mathrm{sgn}(x) = -1$ if $x < 0$.

Analogously, the Fourier transforms of Riemann-Liouville and Riesz fractional integrals are given by

$$\mathcal{F}\{D_{\pm}^{-\alpha} f(x); k\} = (\mp ik)^{-\alpha} \mathcal{F}\{f(x); k\} \quad (0 < \alpha < 1) \tag{12}$$

$$\mathcal{F}\{D^{-\alpha} f(x); k\} = |k|^{-\alpha} \mathcal{F}\{f(x); k\} \quad (0 < \alpha < 1) \tag{13}$$

For order $0 < \alpha \le 2$ and skewness $|\theta| \le \min(\alpha, 2-\alpha)$, the Riesz-Feller derivative is defined as

$$ {}_{x}D_{\theta}^{\alpha} f(x) = \frac{\Gamma(1+\alpha)}{\pi} \left\{ \begin{aligned} &\sin\frac{(\alpha+\theta)\pi}{2} \int_{0}^{\infty} \frac{f(x+\xi)-f(x)}{\xi^{1+\alpha}} d\xi \\ &+\sin\frac{(\alpha-\theta)\pi}{2} \int_{0}^{\infty} \frac{f(x-\xi)-f(x)}{\xi^{1+\alpha}} d\xi \end{aligned} \right\} \tag{14}$$

so that its Fourier transform is

$$\mathcal{F}\{ {}_{x}D_{\theta}^{\alpha} f(x); k\} = -|k|^{\alpha} e^{i\,\mathrm{sgn}(k)\theta\pi/2} \mathcal{F}\{f(x); k\} \quad (0 < \alpha \le 2)$$

3. FRACTIONAL FOKKER-PLANCK EQUATION FOR DRIFT-DIFFUSION MODEL

The fractional Fokker-Planck equation (fFPE)

$$ {}_{t}D_{*}^{\gamma} p(x,t) = -K_{\alpha} c_{\alpha} (D_{+}^{\alpha} + D_{-}^{\alpha}) p(x,t) + K_{\beta}\, {}_{x}D_{\theta}^{\beta} p(x,t) \tag{16}$$

is a generalization of classical drift-diffusion equation that describes drift-diffusion processes, where $p(x,t)$ is the

probability that a particle is found at x at time t or the spatial distribution of fluid density or solute concentration at a particular time. K_α and K_β are the respective coefficients for drift and diffusion. In addition, $0 < \alpha \le 1$ and $1 < \beta \le 2$ are the fractional orders of spatial derivatives, $0 < \gamma \le 1$ is the fractional order of temporal derivative. As a result,

$$D_+^\alpha p(x,t) = \frac{1}{\Gamma(1-\alpha)} \frac{d}{dx} \int_{-\infty}^{x} (x-\xi)^{-\alpha} p(\xi,t) d\xi \qquad (17)$$

$$D_-^\alpha p(x,t) = -\frac{1}{\Gamma(1-\alpha)} \frac{d}{dx} \int_{x}^{+\infty} (\xi-x)^{-\alpha} p(\xi,t) d\xi \qquad (18)$$

and $c_\alpha = -(2\cos(\alpha\pi/2))^{-1}$. Also on the right hand side of Eq.(16), ${}_x D_\theta^\beta$ is the Riesz-Feller derivative of order β. On the left side of Eq.(16), the Caputo time-fractional derivative of order γ is defined as

$${}_t D_*^\gamma p(x,t) = \begin{cases} \dfrac{1}{\Gamma(-\gamma)} \displaystyle\int_0^t (t-\tau)^{-\gamma-1} p(x,\tau) d\tau & (0 < \gamma < 1) \\ \dfrac{d}{dt} p(x,t) & (\gamma = 1) \end{cases} \qquad (19)$$

The Laplace transform of Eq.(19) is

$$\mathcal{L}\{ {}_t D_*^\gamma p(x,t); s\} = s^\gamma \tilde{p}(x,s) - s^{\gamma-1} \tilde{p}(x,0) \qquad (20)$$

Applying Laplace transform to both sides of Eq.(16), we receive

$$s^\gamma \tilde{p}(x,s) - s^{\gamma-1} \tilde{p}(x,0) = -K_\alpha D^\alpha \tilde{p}(x,s) + K_\beta {}_x D_\theta^\beta \tilde{p}(x,s) \qquad (21)$$

Applying Fourier transform further to both sides of Eq.(21) yields

$$\begin{aligned} &s^\gamma \hat{\tilde{p}}(k,s) - s^{\gamma-1} \hat{\tilde{p}}(k,0) = \\ &-K_\alpha \mid k \mid^\alpha \hat{\tilde{p}}(k,s) + K_\beta \mid k \mid^\beta e^{i \operatorname{sgn}(k) \theta \pi/2} \hat{\tilde{p}}(k,s) \end{aligned} \qquad (22)$$

Therefore,

$$\hat{\tilde{p}}(k,s) = \frac{s^{\gamma-1}}{s^\gamma - (K_\beta \mid k \mid^\beta e^{i \operatorname{sgn}(k) \theta \pi/2} - K_\alpha \mid k \mid^\alpha)} \hat{\tilde{p}}(k,0) \qquad (23)$$

The inverse Laplace transform of Eq.(23) is

$$\hat{p}(k,t) = \mathcal{E}_{\gamma,1}(K_\beta \mid k \mid^\beta e^{i \operatorname{sgn}(k) \theta \pi/2} t^\gamma - K_\alpha \mid k \mid^\alpha t^\gamma) \hat{p}(k,0) \qquad (24)$$

where $\mathcal{E}_{\gamma,1}$ is the Mittag-Leffler function of order $(\gamma,1)$. The general Mittag-Leffler function of order (γ,η) is defined as

$$\mathcal{E}_{\gamma,\eta}(z) = \sum_{n=0}^{\infty} \frac{z^n}{\Gamma(\gamma n + \eta)} \qquad (25)$$

The inverse Fourier transform of Eq.(24) is

$$\begin{aligned} p(x,t) &= \frac{1}{2\pi} \int_{-\infty}^{+\infty} e^{-ikx} \mathcal{E}_{\gamma,1}(K_\beta \mid k \mid^\beta e^{i \operatorname{sgn}(k) \theta \pi/2} t^\gamma - K_\alpha \mid k \mid^\alpha t^\gamma) \hat{p}(k,0) dk \\ &= \frac{1}{2\pi} \int_{-\infty}^{+\infty} e^{-ikx} \mathcal{E}_{\gamma,1}(K_\beta \mid k \mid^\beta e^{i \operatorname{sgn}(k) \theta \pi/2} t^\gamma - K_\alpha \mid k \mid^\alpha t^\gamma) \int_{-\infty}^{+\infty} e^{iky} p(y,0) dy dk \\ &= \int_{-\infty}^{+\infty} \frac{1}{2\pi} \int_{-\infty}^{+\infty} e^{-ik(x-y)} \mathcal{E}_{\gamma,1}(K_\beta \mid k \mid^\beta e^{i \operatorname{sgn}(k) \theta \pi/2} t^\gamma - K_\alpha \mid k \mid^\alpha t^\gamma) dk p(y,0) dy \\ &= \int_{-\infty}^{+\infty} G_{\alpha,\beta,\gamma}^\theta (x-y,t) p(y,0) dy \\ &= G_{\alpha,\beta,\gamma}^\theta (x,t) \otimes p(y,0) \end{aligned} \qquad (26)$$

where

$$G_{\alpha,\beta,\gamma}^\theta (x,t) = \frac{1}{2\pi} \int_{-\infty}^{+\infty} e^{-ikx} \mathcal{E}_{\gamma,1}(-K_\alpha \mid k \mid^\alpha t^\gamma + K_\beta \mid k \mid^\beta e^{i \operatorname{sgn}(k) \theta \pi/2} t^\gamma) dk \qquad (27)$$

is the Green or kernel function. Its Fourier transform is

$$\hat{G}_{\alpha,\beta,\gamma}^\theta (k,t) = \mathcal{E}_{\gamma,1}(-K_\alpha \mid k \mid^\alpha t^\gamma + K_\beta \mid k \mid^\beta e^{i \operatorname{sgn}(k) \theta \pi/2} t^\gamma) \qquad (28)$$

The analytical solution in Eq.(26) for fFPE can be approximated by continuous-time random walk or path integrals. Notice that the kernel function in Eq.(27) is a generalization of traditional Gaussian kernel. When $\alpha = 1$, $\beta = 2$, $\gamma = 1$, and $\theta = 0$, the kernel function becomes Gaussian.

The fFPE in Eq.(16) provides a parametric approach to represent model-form uncertainty. Different combinations of α, β, γ, and θ lead to distributions with heavy tails or skewness. Orders α and β capture the uncertainty related to spatial distribution, whereas γ provides the sense of uncertainty in time domain. Skewness θ represents the anisotropic property of diffusion so that dispersion is orientation-dependent.

To provide a sense of how the parameters affect the simulation results, here some plots of probability density functions with different model-form parameters are given. Figure 1 shows the effect of skewness θ, and Figure 2 illustrates the effect of β. More combinations of the parameters are shown in Figure 3.

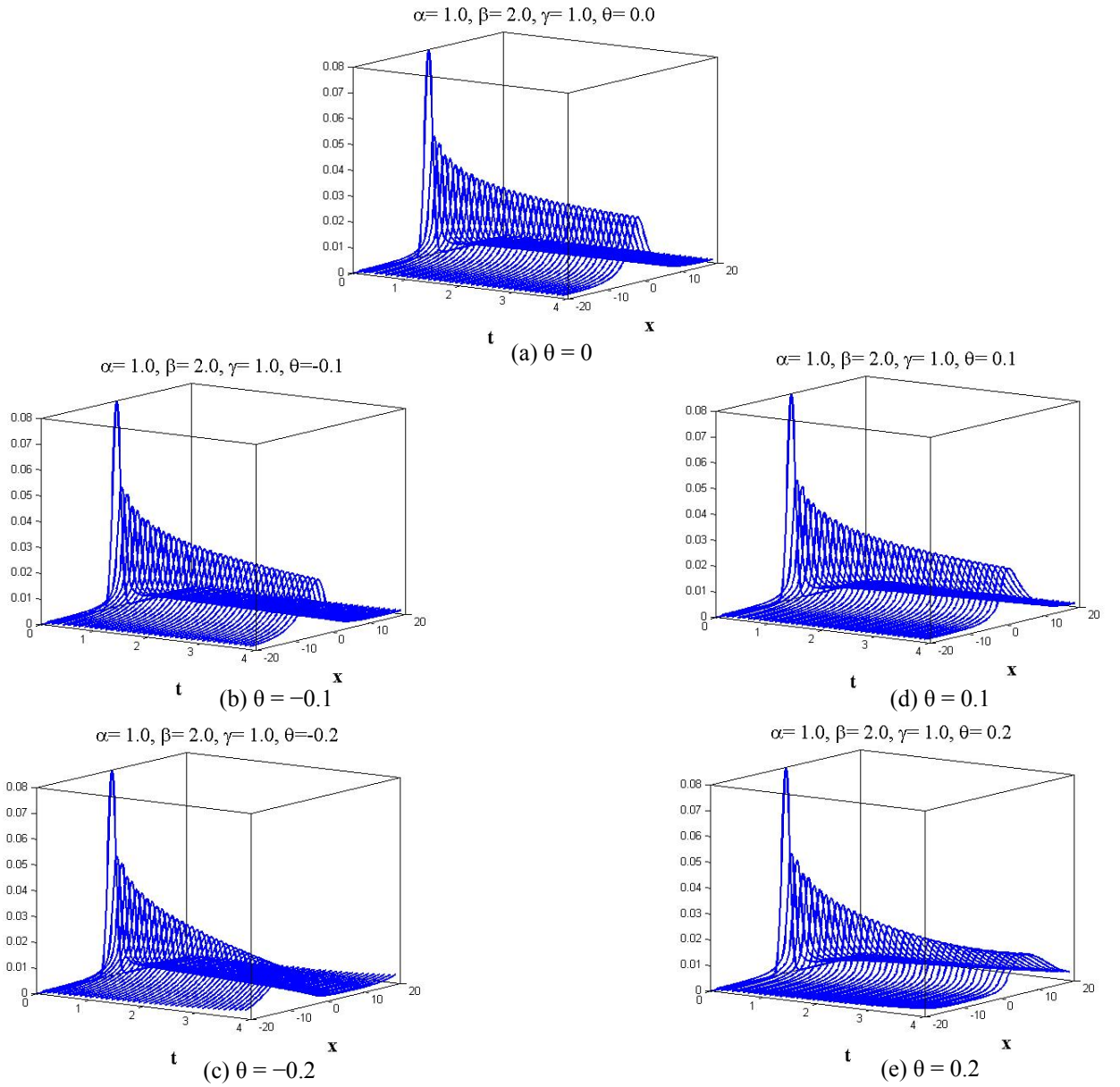

Figure 1: The effect of skewness on probability density functions

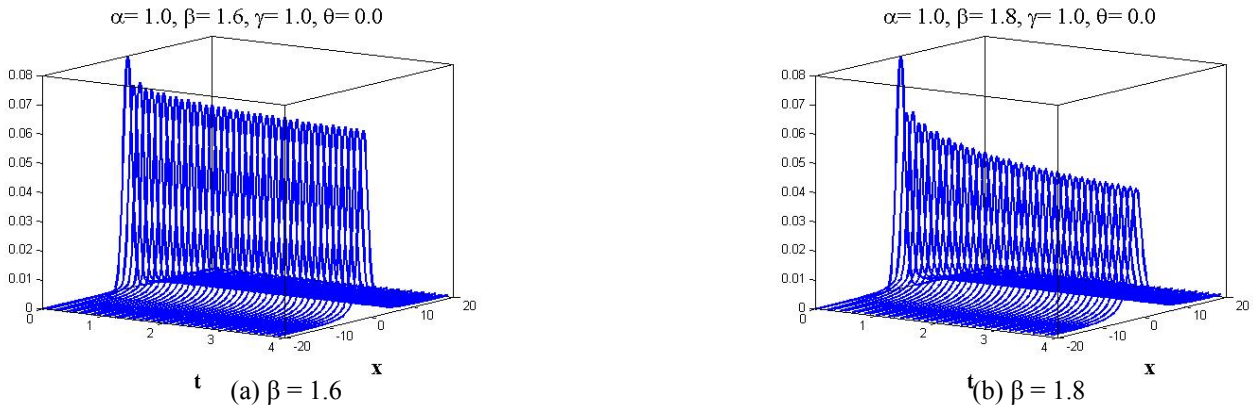

Figure 2: The effect of β on probability density functions

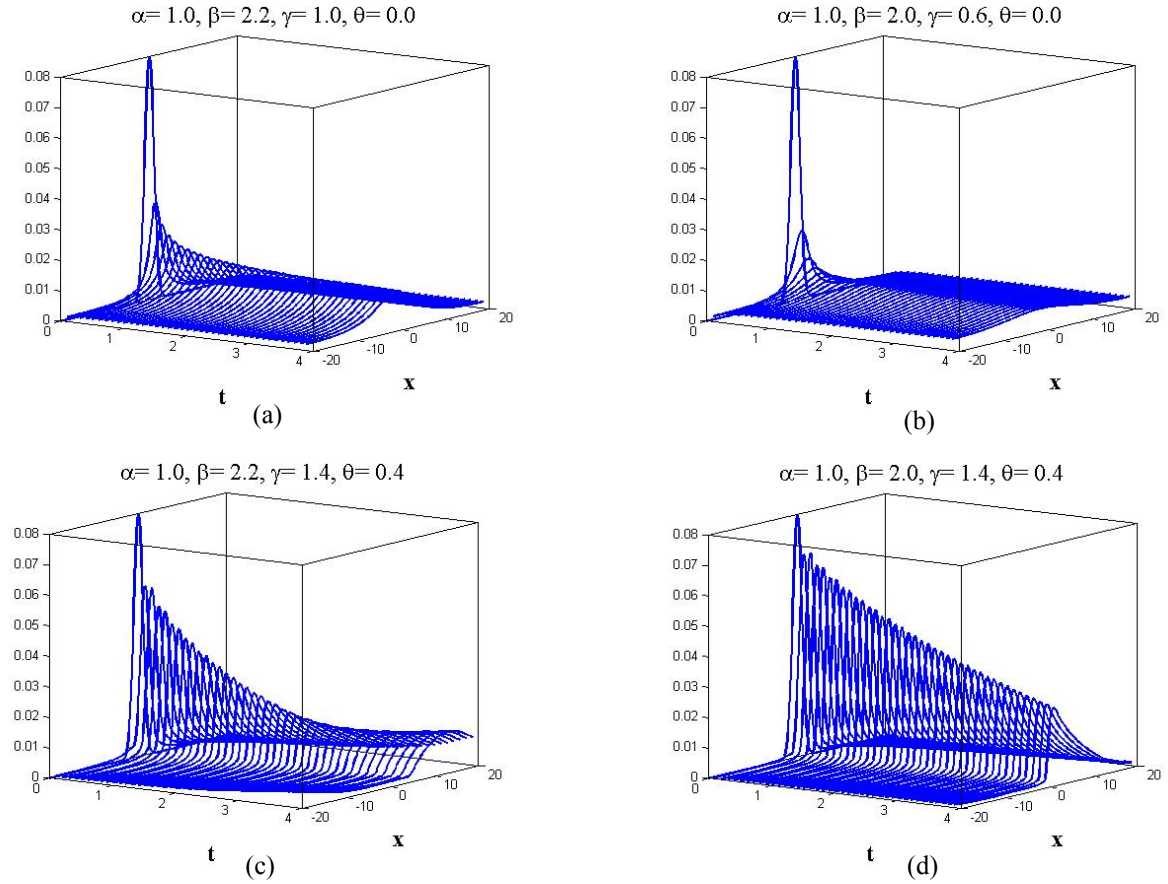

Figure 3: Probability density functions with different combinations of model-form parameters

4. QUANTIFICATION OF MODEL-FORM UNCERTAINTY IN DRIFT-DIFFUSION PROCESSES

As shown in Section 3, model-form parameters α, β, γ, and θ provide a variety of possible probability distributions which cannot be obtained by simply changing drift and diffusion coefficients of classical FPE. The flexibility provides a new approach to quantify model-form uncertainty. In this section, a new approach of model selection based on calibration is proposed, where an optimization formulation is developed to reduce model-form uncertainty. It uses the local sensitivity analysis of model prediction with different model forms.

4.1 Local Sensitivity Analysis

For global sensitivity analysis, we may choose statistical [15] or non-statistical [16] approaches. Here, the local sensitivity of the model prediction in Eq.(26) is analyzed by estimating the first derivatives with respect to the model-form parameters.

If the probability in Eq.(26) is denoted as $P(x,t \mid \Lambda)$ where $\Lambda = (\alpha, \beta, \gamma, \theta)$ is the combination of model-form parameters, then

$$\begin{aligned} \frac{\partial}{\partial \Lambda} P(x,t \mid \Lambda) &= \frac{\partial}{\partial \Lambda} G^{\theta}_{\alpha,\beta,\gamma}(x) \otimes p(y,0) \\ &= \int_{-\infty}^{+\infty} \frac{\partial}{\partial \Lambda} G^{\theta}_{\alpha,\beta,\gamma}(x-y,t) p(y,0) dy \end{aligned} \tag{29}$$

Specifically,

$$\frac{\partial}{\partial \alpha} G^{\theta}_{\alpha,\beta,\gamma}(x,t) = \frac{1}{2\pi} \int_{-\infty}^{+\infty} e^{-ikx} \frac{-\alpha K_{\alpha} \mid k \mid^{\alpha-1}}{\gamma(-K_{\alpha} \mid k \mid^{\alpha} + K_{\beta} \mid k \mid^{\beta} e^{i\,\mathrm{sgn}(k)\theta\pi/2})} \mathcal{E}_{\gamma,0}(-K_{\alpha} \mid k \mid^{\alpha} t^{\gamma} + K_{\beta} \mid k \mid^{\beta} e^{i\,\mathrm{sgn}(k)\theta\pi/2} t^{\gamma}) dk \tag{30}$$

$$\frac{\partial}{\partial\beta}G^{\theta}_{\alpha,\beta,\gamma}(x,t)=\frac{1}{2\pi}\int_{-\infty}^{+\infty}e^{-ikx}\frac{\beta K_{\beta}\mid k\mid^{\beta-1}\ e^{i\,\mathrm{sgn}(k)\theta\pi/2}}{\gamma(-K_{\alpha}\mid k\mid^{\alpha}+K_{\beta}\mid k\mid^{\beta}\ e^{i\,\mathrm{sgn}(k)\theta\pi/2})}\mathcal{E}_{\gamma,0}(-K_{\alpha}\mid k\mid^{\alpha}\ t^{\gamma}+K_{\beta}\mid k\mid^{\beta}\ e^{i\,\mathrm{sgn}(k)\theta\pi/2}t^{\gamma})dk \tag{31}$$

$$\frac{\partial}{\partial\gamma}G^{\theta}_{\alpha,\beta,\gamma}(x,t)=\frac{1}{2\pi}\int_{-\infty}^{+\infty}e^{-ikx}t^{-1}\mathcal{E}_{\gamma,0}(-K_{\alpha}\mid k\mid^{\alpha}\ t^{\gamma}+K_{\beta}\mid k\mid^{\beta}\ e^{i\,\mathrm{sgn}(k)\theta\pi/2}t^{\gamma})dk \tag{32}$$

$$\frac{\partial}{\partial\theta}G^{\theta}_{\alpha,\beta,\gamma}(x,t)=\frac{1}{2\pi}\int_{-\infty}^{+\infty}e^{-ikx}\frac{i\,\mathrm{sgn}(k)\frac{\pi}{2}K_{\beta}\mid k\mid^{\beta}\ e^{i\,\mathrm{sgn}(k)\theta\pi/2}}{\gamma(-K_{\alpha}\mid k\mid^{\alpha}+K_{\beta}\mid k\mid^{\beta}\ e^{i\,\mathrm{sgn}(k)\theta\pi/2})}\mathcal{E}_{\gamma,0}(-K_{\alpha}\mid k\mid^{\alpha}\ t^{\gamma}+K_{\beta}\mid k\mid^{\beta}\ e^{i\,\mathrm{sgn}(k)\theta\pi/2}t^{\gamma})dk \tag{33}$$

The respective Fourier transforms are

$$\mathcal{F}\{\frac{\partial}{\partial\alpha}G^{\theta}_{\alpha,\beta,\gamma}(x,t);k\}=\frac{-\alpha K_{\alpha}\mid k\mid^{\alpha-1}}{\gamma(-K_{\alpha}\mid k\mid^{\alpha}+K_{\beta}\mid k\mid^{\beta}\ e^{i\,\mathrm{sgn}(k)\theta\pi/2})}\mathcal{E}_{\gamma,0}(-K_{\alpha}\mid k\mid^{\alpha}\ t^{\gamma}+K_{\beta}\mid k\mid^{\beta}\ e^{i\,\mathrm{sgn}(k)\theta\pi/2}t^{\gamma}) \tag{34}$$

$$\mathcal{F}\{\frac{\partial}{\partial\beta}G^{\theta}_{\alpha,\beta,\gamma}(x,t);k\}=\frac{\beta K_{\beta}\mid k\mid^{\beta-1}\ e^{i\,\mathrm{sgn}(k)\theta\pi/2}}{\gamma(-K_{\alpha}\mid k\mid^{\alpha}+K_{\beta}\mid k\mid^{\beta}\ e^{i\,\mathrm{sgn}(k)\theta\pi/2})}\mathcal{E}_{\gamma,0}(-K_{\alpha}\mid k\mid^{\alpha}\ t^{\gamma}+K_{\beta}\mid k\mid^{\beta}\ e^{i\,\mathrm{sgn}(k)\theta\pi/2}t^{\gamma}) \tag{35}$$

$$\mathcal{F}\{\frac{\partial}{\partial\gamma}G^{\theta}_{\alpha,\beta,\gamma}(x,t);k\}=t^{-1}\mathcal{E}_{\gamma,0}(-K_{\alpha}\mid k\mid^{\alpha}\ t^{\gamma}+K_{\beta}\mid k\mid^{\beta}\ e^{i\,\mathrm{sgn}(k)\theta\pi/2}t^{\gamma}) \tag{36}$$

$$\mathcal{F}\{\frac{\partial}{\partial\theta}G^{\theta}_{\alpha,\beta,\gamma}(x,t);k\}=\frac{i\,\mathrm{sgn}(k)\frac{\pi}{2}K_{\beta}\mid k\mid^{\beta}\ e^{i\,\mathrm{sgn}(k)\theta\pi/2}}{\gamma(-K_{\alpha}\mid k\mid^{\alpha}+K_{\beta}\mid k\mid^{\beta}\ e^{i\,\mathrm{sgn}(k)\theta\pi/2})}\mathcal{E}_{\gamma,0}(-K_{\alpha}\mid k\mid^{\alpha}\ t^{\gamma}+K_{\beta}\mid k\mid^{\beta}\ e^{i\,\mathrm{sgn}(k)\theta\pi/2}t^{\gamma}) \tag{37}$$

Notice that [17]

$$\frac{d}{dz}\mathcal{E}_{\gamma,\eta}(z)=\frac{\mathcal{E}_{\gamma,\eta-1}(z)-(\eta-1)\mathcal{E}_{\gamma,\eta}(z)}{\gamma z}$$

Therefore,

$$\frac{d}{dz}\mathcal{E}_{\gamma,1}(z)=\frac{\mathcal{E}_{\gamma,0}(z)}{\gamma z}$$

The sensitivity formulation is used in the calibration process described in the following section.

4.2 Model Form Calibration

Here a new approach for model calibration is proposed, which is based on mutual information. Given two random variables X and Y, the mutual information of the two variables is defined as

$$I(X,Y)=\int\int p(X,Y)\log\frac{p(X,Y)}{p(X)p(Y)}dXdY \tag{38}$$

The new calibration process is based on the criteria of the maximum accumulative mutual information between the model prediction and experimental observation. Given the model prediction $p(x,t)$ from a particular form and the observation $p(z,t)$ from experiment, the *accumulative mutual information* between the two is defined as

$$\mathcal{M}(x,z)=\int\int\int p(x,z,t)\log\frac{p(x,z,t)}{p(x,t)p(z,t)}dxdzdt \tag{39}$$

where the joint probability

$$p(x,z,t)=p(z\mid x,t)p(x,t) \tag{40}$$

Here, the likelihood $p(x\mid z,t)$ characterizes the difference between the observation and model prediction. The likelihood is

$$\begin{aligned}p(z\mid x,t)&=\int_{-\infty}^{+\infty}G^{\theta}_{\alpha,\beta,\gamma}((x-z)-y,t)p(y,0)dy\\&=G^{\theta}_{\alpha,\beta,\gamma}(x-z)\otimes p(y,0)\\&=P(x-z,t\mid\Lambda)\end{aligned} \tag{41}$$

The proposed criteria for model calibration is to find the optimum parameters α, β, γ, and θ as the solution of

$$\max_{\alpha,\beta,\gamma,\theta}\mathcal{M}(x,z) \tag{42}$$

Given Eqs.(26) and (40), the accumulative mutual information in Eq.(39) becomes

$$\begin{aligned}&\mathcal{M}(x,z)\\&=\iiint p(z\mid x,t)p(x,t)\log\frac{p(z\mid x,t)}{p(z,t)}dxdzdt\\&=\iiint\left[\log\frac{\left(G^{\theta}_{\alpha,\beta,\gamma}(x-z,t)\otimes p(y,0)\right)\left(G^{\theta}_{\alpha,\beta,\gamma}(x,t)\otimes p(y,0)\right)}{p(z,t)}\right]dxdzdt\\&=\iiint\left[P(x-z,t\mid\Lambda)P(x,t\mid\Lambda)\log\frac{P(x-z,t\mid\Lambda)}{p(z,t)}\right]dxdzdt\end{aligned} \tag{43}$$

The local search direction to find the optimum solution of Eq.(42) is the first derivative of Eq.(43) with respect to the model-form parameters, which is

$$\frac{\partial}{\partial\Lambda}\mathcal{M}(x,z)$$
$$=\iiint\left[\begin{array}{l}P(x,t\mid\Lambda)\left[1+\log\frac{P(x-z,t\mid\Lambda)}{p(z,t)}\right]\frac{\partial}{\partial\Lambda}P(x-z,t\mid\Lambda)\\+P(x-z,t\mid\Lambda)\log\frac{P(x-z,t\mid\Lambda)}{p(z,t)}\frac{\partial}{\partial\Lambda}P(x,t\mid\Lambda)\end{array}\right]dxdzdt \tag{44}$$

Notice that

$$\frac{\partial}{\partial\Lambda}P(x-z,t\mid\Lambda)=\frac{\partial}{\partial\Lambda}G^{\theta}_{\alpha,\beta,\gamma}(x-z)\otimes p(y,0) \tag{45}$$

which is similar to Eq.(29). The calibration process will follow the algorithm of optimization in Table 1. A simplified version of calibration is obviously based on mutual information instead of accumulative mutual information in Eq.(39).

A numerical example is used to demonstrate the proposed calibration procedure. 2,000 samples are randomly drawn from a Gaussian distribution. The simpler criterion of maximizing mutual information is applied. The pdf of experimental data is shown with the solid line with markers in Figure 4. An initial set of parameters ($\alpha=1$, $\beta=2.2$, $\gamma=0.8$, and $\theta=0.4$) are first given and the corresponding pdf is shown as the dash line in Figure 4. After 250 iterations of searching procedure in the algorithm in Table 1, the updated and final pdf are shown as the solid lines in Figure 4. The optimized parameters are $\alpha=1$, $\beta=2.202$, $\gamma=1.571$, and $\theta=0.811$. The search history of γ and θ is shown in Figure 5. The value of mutual information gradually increases until it converges, as shown in Figure 6.

Notice that the number of iterations is directly related to the threshold value ε in the stop criteria as well as the step size λ during the search. The threshold value used in Figure 6(a) is 5e−6 and the step size is 1.0. A larger threshold value or a larger step size will lead to fewer iterations. For instance, when the step size is increased to 2.0, the number of iterations is reduced to 109 with the same threshold value, as shown in Figure 6(b).

Table 1: The algorithm of model calibration

1.	Provide the distribution $p(z,t)$ from observation data;
2.	Provide an initial guess of Λ ;
3.	Calculate $P(x,t\mid\Lambda)$ based on Eq.(26);
4.	Calculate $P(x-z,t\mid\Lambda)$ based on Eq.(41);
5.	Calculate $\partial\mathcal{M}/\partial\Lambda$ based on Eq.(44);
6.	IF $\mid\partial\mathcal{M}/\partial\Lambda\mid>\varepsilon$
7.	Choose a step size λ, $\Lambda\leftarrow\Lambda+\lambda(\partial\mathcal{M}/\partial\Lambda)$;
8.	Go to Step 3;
9.	ELSE
10.	Stop.

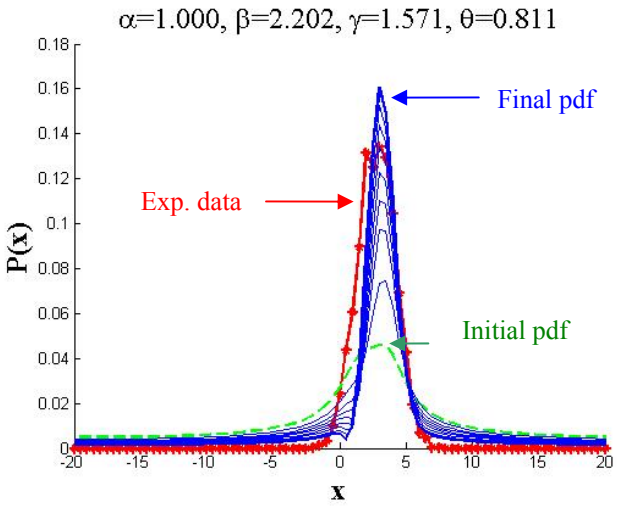

Figure 4: Probability density functions (pdf's) evolved in the calibration process against a Gaussian distribution

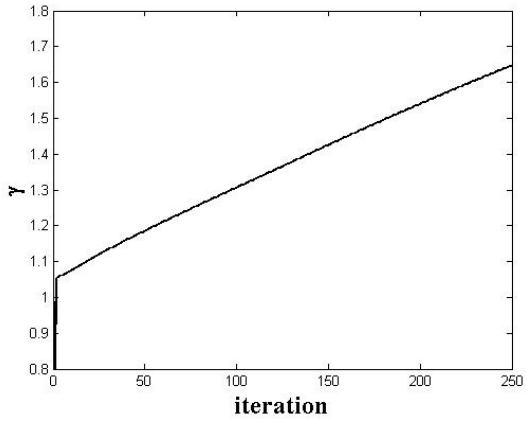

(a) γ

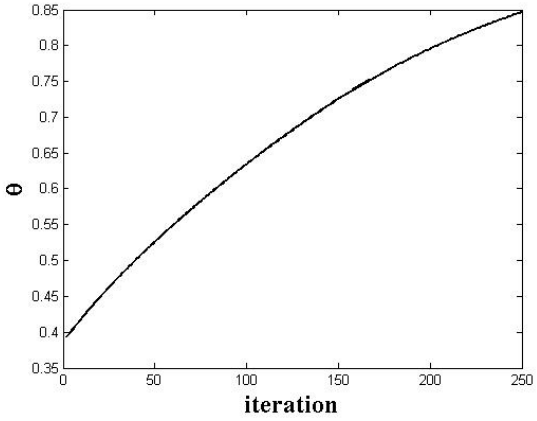

(b) θ

Figure 5: The search history of model-form parameters in the calibration process

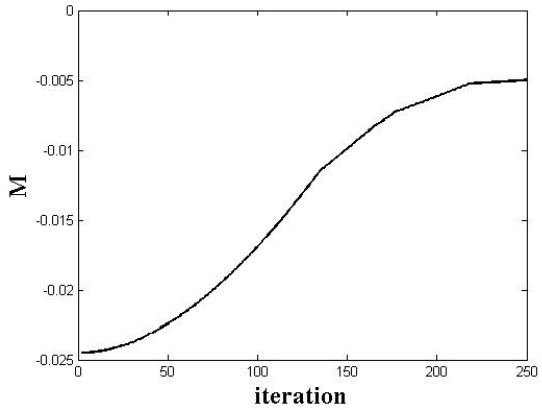

(a) step size $\lambda = 1.0$

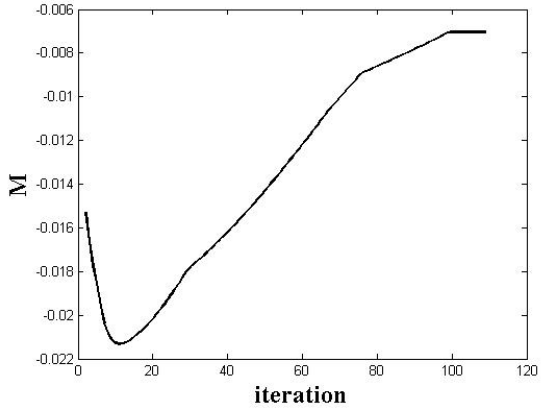

(b) step size $\lambda = 2.0$

Figure 6: The search history of mutual information with different step sizes for Gaussian distribution

The proposed calibration approach can also be applied dynamically as an incremental calibration procedure when data are collected sequentially and the model can be re-estimated accordingly.

Compared to Bayesian model average, there is no need to assume the probabilities associated with different model choices. The calibration process is continuous for model-form parameters.

The second example is to calibrate the model against a Fréchet distribution with the pdf as

$$f(x) = \begin{cases} 0 & (x < \mu - \frac{\sigma}{\xi}) \\ \sigma^{-1}[1+\xi(\frac{x-\mu}{\sigma})]^{-1-1/\xi} \exp\{-[1+\xi(\frac{x-\mu}{\sigma})]^{-1/\xi}\} & otherwise \end{cases}$$

with parameters $\mu = 0.0$, $\sigma = 1.0$, and $\xi = 0.5$. The result of calibration is shown in Figure 7, where the solid line with star markers denotes the pdf of Fréchet distribution, the dash line is the initial pdf, and the solid lines show the update process of calibrated pdf. The change of accumulative mutual information is shown in Figure 8.

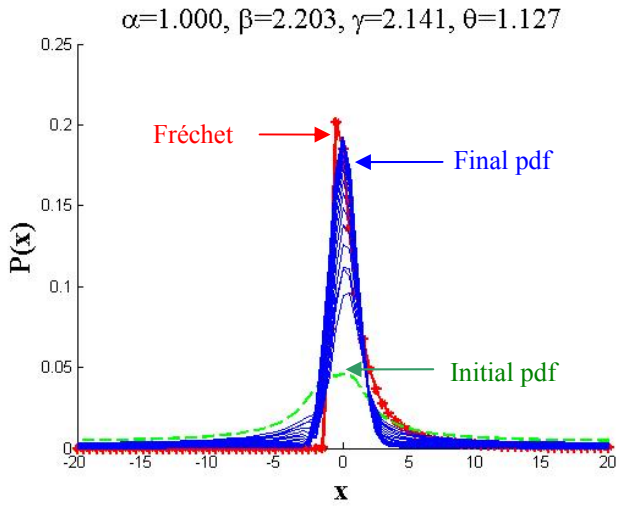

Figure 7: Probability density functions (pdf's) evolved in the calibration process against a Fréchet distribution

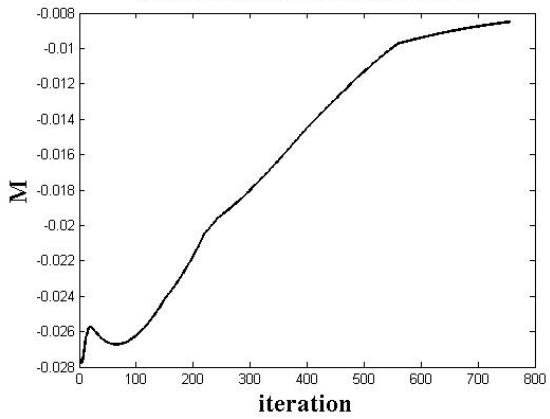

Figure 8: The search history of mutual information for Fréchet distribution

5. DISCUSSIONS AND CONCLUSION

The method to quantify model-form uncertainty in simulating drift-diffusion phenomena is generic enough to capture the advection-diffusion and probability evolution driven by complex physical mechanisms. Therefore, the modeled processes are not restricted to Gaussian any more. Long-range correlations and memory effects are commonly observed in physical world. The simplification involved in Gaussian process modeling has inherent errors in its description. Fractional calculus provides a versatile tool to quantify and reduce the model-form uncertainty.

Except for a few simple pdf's that have analytical forms subject to fractional operators, most of fractional integrals and derivatives have to rely on numerical approaches to estimate. Fractional derivatives can be approximated by series of integer-order derivatives [18,3], integer-order moments [19,20], or

finite difference [9]. The general analytical solution provided in Section 3 enables us to employ other numerical methods to find the solution. Numerical method is not the focus of this paper. Yet the approximated solutions obtained in the paper are based on fast Fourier transform with relatively low computational costs.

It is seen in Section 4.2 that the model calibration works well for some classical distributions. However, it should be aware that the four model-form parameters are not completely independent. It leads to the possibility that multiple optimum combinations of parameters produce the same distributions. This issue will become less apparent when multiple time steps of probability evolution are involved in the calibration process.

In the future work, numerical methods to enhance both the efficiency and accuracy for approximated solutions need to be studied. The discretization in real and reciprocal spaces for fast Fourier transform requires a large number of values to reduce the approximation error. A combination of approximations in real and functional spaces may improve the efficiency by reducing the density of discretization. How to incorporate multiple time steps efficiently in model calibration also requires more investigation.

REFERENCES

[1] Xiu, D. (2010). *Numerical Methods for Stochastic Computations: A Spectral Method Approach*, Princeton: Princeton University Press.

[2] Ghanem, R. G., & Spanos, P. D. (1991). *Stochastic finite elements: a spectral approach*. New York: Springer-Verlag.

[3] Samko, S. G., Kilbas, A. A., & Marichev, O. I. (1993). *Fractional Integrals and Derivatives: Theory and Applications*. Gordon and Breach Science Publishers, Yverdon.

[4] Miller, K. S., & Ross, B. (1993). *An introduction to the fractional calculus and fractional differential equations*. Wiley Interscience.

[5] Tenreiro Machado, J. A., Silva, M. F., Barbosa, R. S., Jesus, I. S., Reis, C. M., Marcos, M. G., & Galhano, A. F. (2010). Some applications of fractional calculus in engineering. *Mathematical Problems in Engineering*, 2010, 639801.

[6] Carpinteri, A., Chiaia, B., & Cornetti, P. (2003). On the mechanics of quasi-brittle materials with a fractal microstructure. *Engineering Fracture Mechanics*, **70**(16), 2321-2349.

[7] Lazopoulos, K. A. (2006). Non-local continuum mechanics and fractional calculus. *Mechanics Research Communications*, **33**(6), 753-757.

[8] Mainardi, F., Luchko, Y., & Pagnini, G. (2001). The fundamental solution of the space-time fractional diffusion equation. *Fractional Calculus and Applied Analysis*, **4**(2), 153-192.

[9] Liu, Q., Liu, F., Turner, I.W., & Anh, V.V. (2007). Approximation of the Lévy–Feller advection–dispersion process by random walk and finite difference method. *Journal of Computational Physics*, **222**(1), 57-70.

[10] Fogedby, H. C. (1994). Lévy flights in random environments. *Physical Review Letters*, **73**(19), 2517.

[11] Di Paola, M. (2014). Fokker Planck equation solved in terms of complex fractional moments. *Probabilistic Engineering Mechanics*, **38**, 70-76.

[12] Laskin, N. (2000). Fractional quantum mechanics and Lévy path integrals. *Physics Letters A*, **268**(4), 298-305.

[13] Jenkinson, A. F. (1955). The frequency distribution of the annual maximum (or minimum) values of meteorological elements. *Quarterly Journal of the Royal Meteorological Society*, **81**(348), 158-171.

[14] Hosking, J. R. M., Wallis, J. R., & Wood, E. F. (1985). Estimation of the generalized extreme-value distribution by the method of probability-weighted moments. *Technometrics*, **27**(3), 251-261.

[15] Saltelli, A., Ratto, M., Andres, T., Campolongo, F., Cariboni, J., Gatelli, D., Saisana, M., and Tarantola, S., (2008) *Global Sensitivity Analysis: The Primer*. Wiley-Interscience

[16] Hu, J., Wang, Y., Cheng, A., & Zhong, Z. (2015) Sensitivity analysis in quantified interval constraint satisfaction problems. *Journal of Mechanical Design* (in press)

[17] Gorenflo, R., Loutchko, J., and Luchko, Y. (2002) Computation of the Mittag-Leffler function $E_{\alpha,\beta}(z)$ and its derivative. *Fractional Calculus and Applied Analysis*, **5**(4), 491-518.

[18] Atanacković, T. M., Konjik, S., & Pilipović, S. (2008). Variational problems with fractional derivatives: Euler–Lagrange equations. *Journal of Physics A: Mathematical and Theoretical*, **41**(9), 095201.

[19] Djordjevic, V. D., & Atanackovic, T. M. (2008). Similarity solutions to nonlinear heat conduction and Burgers/Korteweg–deVries fractional equations. *Journal of Computational and Applied Mathematics*, **222**(2), 701-714.

[20] Pooseh, S., Almeida, R., & Torres, D. F. (2013). Numerical approximations of fractional derivatives with applications. *Asian Journal of Control*, **15**(3), 698-712.